

# Di-Vector Boson + Jet Production via Gluon Fusion at Hadron Colliders

Pankaj Agrawal <sup>\*</sup> and Ambresh Shivaji <sup>†</sup>  
 Institute of Physics, Sainik School Post, Bhubaneswar 751 005, India

## Abstract

We study the production of two electro-weak vector bosons in association with a jet via gluon fusion. In particular we consider the production of  $\gamma Zg$ ,  $ZZg$  and  $W^+W^-g$  at hadron colliders and compute their cross-sections. Such processes have already produced large number of events at the Large Hadron Collider (LHC) by now. These processes can be background to the Higgs boson production and a number of beyond the standard model scenarios. Therefore it is important to know the values of their contribution. The calculation is based on conventional Feynman diagram approach. In particular we find that the process  $gg \rightarrow ZZg$  can make a significant contribution to the process  $pp \rightarrow ZZ + \text{jet}$ .

## 1 Introduction

The search for new physics at the LHC is in progress and the collider is delivering data presently at 8 TeV centre-of-mass energy. The discovery of a fundamental scalar particle (most probably a Higgs boson) of mass around 125 GeV has received a lot of world-wide attention [1]. We expect more good news from the experiments at the LHC before the collider goes for a two years long pause. So far, the standard model (SM) of particle physics seems to be in excellent agreement with the collected data (more than  $10 \text{ fb}^{-1}$ ). There has been searches for the hints of physics beyond the SM such as supersymmetry, large extra dimensions, etc. But, as of now, there is no clear evidence [2]. The process of identifying the discovered fundamental scalar particle as *the Higgs boson* is also continuing. With the lack of signals for beyond the SM scenarios, there is a need to look for the SM processes that were not accessible earlier at the Tevatron. Most of such processes have several particles in the final state, and/or occur at the higher order. Such processes can also contribute to the background to the new physics signals. One such class of processes is multi vector boson production in association with one or more jets.

At the LHC centre-of-mass energy, the collider has another useful feature. In the proton-proton collisions, the gluon luminosity can be quite significant. It can even dominate over the quark luminosity in certain kinematic domains. Therefore, at the LHC, loop mediated gluon fusion processes can be important. Di-vector boson production via gluon fusion have been studied by many authors [3, 4, 5, 6, 7, 8, 9, 10, 11, 12, 14, 15, 16]. We consider another class of processes  $gg \rightarrow VV'g$ , where  $V$  and  $V'$  can be any allowed combination of electro-weak vector bosons. These processes can be a background to Higgs boson production as well as new physics scenarios such as technicolor. At the leading order, these processes receive contribution from quark loop diagrams. The prototype diagrams are displayed in Fig (1). The computation for the process  $gg \rightarrow \gamma\gamma g$  has already been performed [17, 18]. Preliminary results

---

<sup>\*</sup>email:agrawal@iopb.res.in

<sup>†</sup>email:ambresh@iopb.res.in

for  $gg \rightarrow \gamma Zg$  were presented in [19]. Recently, *Melia et al.* have presented calculation for  $gg \rightarrow W^+W^-g$  [20]. In this brief report we present our results for the production of  $\gamma Zg$ ,  $ZZg$  and  $W^+W^-g$  at hadron colliders. Detailed analysis of these processes will be reported in future publications.

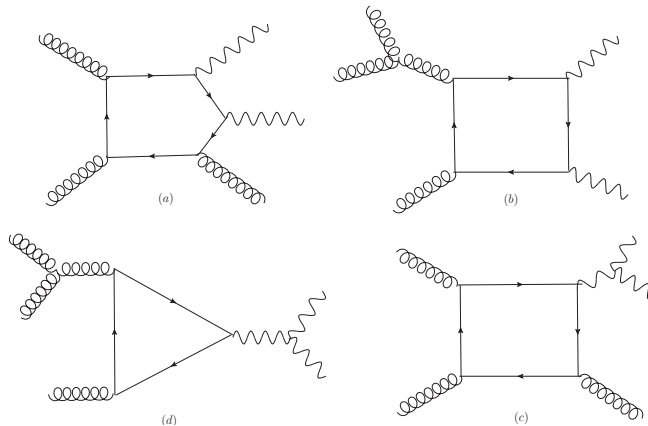


Figure 1: The prototype diagrams for the processes  $gg \rightarrow VV'g$ . The wavy lines represent the appropriate combination of the  $\gamma$ ,  $W$ , or  $Z$  boson. The last two classes (c) and (d) are relevant to  $WWg$  production only. We do not consider diagrams involving Higgs boson for the  $ZZg$  and  $WWg$  cases.

## 2 The Process: $gVV'$

The process  $gg \rightarrow VV'g$  contribute to the cross-section of the process  $pp \rightarrow VV' + \text{jet}$  at NNLO in  $\alpha_s$ . As discussed, although they occur at the one-loop level, their cross-sections can be significant due to large gluon luminosity at the LHC. The processes  $\gamma Zg$  and  $ZZg$  receive contribution from two main classes of quark-loop diagrams – pentagon and box type, as shown in (a) and (b) of Fig (1). Box class of diagrams are due to the triple gluon vertices; they can be further divided into three sub-classes. This sub-classification has it's own physical importance. These are separately gauge invariant with respect to the electro-weak vector bosons. Other diagrams can be obtained by suitable permutation of external legs. For each quark flavor, there are 24 pentagon-type and 18 box-type diagrams. Due to Furry's theorem, only half of the 42 diagrams are independent. Also pentagon diagrams give both vector as well as axial-vector contributions while box diagrams give only vector contribution. We work with five massless quark flavors and expect decoupling of the top quark.

In the case of  $WWg$  process, instead of single quark flavor, two quark flavors of a single generation contribute to the above discussed pentagon and box diagrams. To keep matter simple, for this process, we work with first two generations of massless quarks. It is expected that the contribution from the third generation would not be significant in low  $P_T$  region [16]. There are additional box and triangle class of diagrams due to  $\gamma/Z W^+W^-$  vertex for each quark flavor. These are shown in (c) and (d) of Fig. (1). Due to Furry's theorem, the triangle diagrams with  $\gamma W^+W^-$  coupling don't contribute and only axial part of the triangle diagrams with  $ZW^+W^-$  coupling contribute to the amplitude. Since the axial coupling of  $Z$ - boson to quark is proportional to  $T_3^{(q)}$  value, the axial contributions from additional triangle and box diagrams, when summed over massless quark generation, vanish. The vector contribution of additional box-type diagrams is separately gauge invariant. Because of its color structure, it interferes with the axial part of the pentagon amplitude. We have explicitly checked that its contribution towards total cross-section is very small; therefore we have dropped this contribution. Thus, effectively we are left

with  $ZZg$  like contributions for  $WWg$ . The Higgs boson interference effects for the cases of  $ZZg$  and  $WWg$  are ignored in the present calculation. Our one loop processes, being the leading order processes, are expected to be finite, i.e. free from UV and IR divergences.

The amplitude for our process has the following general structure

$$\begin{aligned}\mathcal{M}^{abc}(gg \rightarrow VV'g) &= i\frac{f^{abc}}{2}\mathcal{M}_V(VV'g) + \frac{d^{abc}}{2}\mathcal{M}_A(VV'g), \\ \mathcal{M}_V(VV'g) &= -e^2g_s^3 C_V(VV'g) (\mathcal{P}_V - \mathcal{B}_V), \\ \mathcal{M}_A(VV'g) &= -e^2g_s^3 C_A(VV'g) (\mathcal{P}_A).\end{aligned}\tag{1}$$

$\mathcal{M}_{V,A}$  are amplitudes for the vector and axial-vector parts of the full amplitude under consideration. Because of Bose symmetry  $\mathcal{M}_V \rightarrow -\mathcal{M}_V$  under exchange of any two external gluons while  $\mathcal{M}_A$  remains same.  $\mathcal{B}_V$  and  $\mathcal{P}_{V,A}$  are box and pentagon contributions from a single flavor (single generation for  $WWg$  case) of quarks. The structure of the amplitude suggests that the vector and axial-vector contributions should be separately gauge invariant. Moreover due to the color structure when we square the amplitude, the interference between the axial and vector contribution vanishes, *i.e.*

$$|\mathcal{M}(gg \rightarrow VV'g)|^2 = \left(6|\mathcal{M}_V|^2 + \frac{10}{3}|\mathcal{M}_A|^2\right).\tag{2}$$

Therefore the cross-section of the process is an incoherent sum of the vector and axial-vector contributions. The couplings  $C_{V,A}$  for various cases are listed below. Contributions from all the relevant quark flavors (described above) are included appropriately.

$$\begin{aligned}C_V(\gamma\gamma g) &= \frac{11}{9}, \quad C_A(\gamma\gamma g) = 0, \\ C_V(\gamma Zg) &= \frac{1}{\sin\theta_w\cos\theta_w} \left(\frac{7}{12} - \frac{11}{9}\sin^2\theta_w\right), \\ C_A(\gamma Zg) &= \frac{1}{\sin\theta_w\cos\theta_w} \left(-\frac{7}{12}\right), \\ C_V(ZZg) &= \frac{1}{\sin^2\theta_w\cos^2\theta_w} \left(\frac{5}{8} - \frac{7}{6}\sin^2\theta_w + \frac{11}{9}\sin^4\theta_w\right), \\ C_A(ZZg) &= \frac{1}{\sin^2\theta_w\cos^2\theta_w} \left(-\frac{5}{8} + \frac{7}{6}\sin^2\theta_w\right), \\ C_V(WWg) &= \frac{1}{\sin^2\theta_w} \left(\frac{1}{2}\right), \\ C_A(WWg) &= \frac{1}{\sin^2\theta_w} \left(-\frac{1}{2}\right).\end{aligned}\tag{3}$$

### 3 Calculation and Numerical Checks

For each class of diagrams, we write down the prototype amplitudes using the SM Feynman rules [21]. The amplitude of all other diagrams are generated by appropriately permuting the external momenta and polarizations in our code. The quark loop traces without  $\gamma_5$  are calculated in  $n$ -dimensions while those with  $\gamma_5$  are calculated in 4-dimensions using FORM [22]. We do not need any  $n$ -dimensional prescription for  $\gamma_5$  as both pentagon and box diagrams are free of anomaly. The amplitude contains tensor loop

integrals. In the case of pentagon-type diagrams, the most complicated integral is rank-5 tensor integral ( $E^{\mu\nu\rho\sigma\delta}$ ); while for the box-type diagrams, rank-4 tensor integral ( $D^{\mu\nu\rho\sigma}$ ) is the most complicated one

$$E^{\mu\nu\rho\sigma\delta} = \int \frac{d^n k}{(2\pi)^n} \frac{k^\mu k^\nu k^\rho k^\sigma k^\delta}{N_0 N_1 N_2 N_3 N_4}, \quad (4)$$

$$D^{\mu\nu\rho\sigma} = \int \frac{d^n k}{(2\pi)^n} \frac{k^\mu k^\nu k^\rho k^\sigma}{N_0 N_1 N_2 N_3}. \quad (5)$$

Here,  $N_i = k_i^2 - m_q^2 + i\epsilon$  and  $k_i$  is the momentum of the  $i^{\text{th}}$  internal line in the corresponding scalar integrals.  $n = (4 - 2\epsilon)$  and  $m_q$  is the mass of the quark in the loop. Five point tensor and scalar integrals are written in terms of box tensor and scalar integrals using 4-dimensional Schouten Identity. For example, a five point scalar integral, in 4-dimensions, can be expressed in terms of five box scalar integrals [24]

$$E_0(0, 1, 2, 3, 4) = \sum_{i=0}^4 c_i D_0^{(i)}, \quad (6)$$

where  $D_0^{(i)}$  is the box scalar integral obtained after removing the  $i^{\text{th}}$  propagator in  $E_0$ . Any  $O(\epsilon)$  correction to the above relation in  $n = (4 - 2\epsilon)$ - dimensions does not contribute to our amplitude. This is because the contributions of the pentagon-type diagrams are UV finite and we have regulated mass singularities by giving small mass to the quarks. The box tensor integrals are reduced into the standard scalar integrals –  $A_0$ ,  $B_0$ ,  $C_0$  and  $D_0$  using FORTRAN routines that follows from the reduction scheme developed by Oldenborgh and Vermaseren [23]. Thus we require box scalar integrals with two massive external legs, at the most. The scalar integrals with massive internal lines are calculated using OneLoop library [25]. Because of very large and complicated expression of the amplitude, we calculate the amplitude numerically before squaring it. This requires numerical evaluation of the polarization vectors of gauge bosons. We choose real basis, instead of helicity basis for the polarization vectors to calculate the amplitude. This is to reduce the size of compiled program and the time taken in running the code. We have used RAMBO to generate three particle phase-space for our processes [26].

The processes  $gg \rightarrow VV'g$  are leading order one-loop processes. The full amplitude in (1) should be both UV as well as IR finite. However, individual diagrams may be UV and/or IR divergent. IR divergence is relevant to only light quark cases. All these singularities are encoded in various scalar integrals. To make UV and IR finiteness check on our amplitude we have derived all the required scalar integrals (up to box scalar integrals with two massive external legs) analytically following t'Hooft and Veltman [27]. We regulate the UV divergence of the scalar integrals using dimensional regularization and infrared singularities by using small quark mass (the mass regularization). Our results are in agreement with those given in [28]. We have verified that our amplitude is both UV and IR finite and it's gauge invariant with respect to all the gluons. Pentagon and box amplitudes are separately gauge invariant with respect to the electro-weak vector bosons. As a consistency check we have also verified that the amplitude vanishes in the large quark-mass limit [29].

## 4 Numerical Results

We have computed the amplitude numerically using the real polarization vector basis. There are 48 polarized amplitudes for the case of  $\gamma Zg$  while 72 for the cases of  $ZZg$  and  $WWg$ . Given the number of diagrams, the number of polarization combination and the length of the amplitude, we have to run the code in parallel environment using a PVM implementation of the VEGAS algorithm [30, 31]. We have

used more than 30 cores to run the code in parallel environment. Still it takes more than eight hours to get suitable cross-section for a given process.

In such loop calculations, there is an issue of numerical instabilities due to large cancellations in the evaluation of the scalar and tensor integrals. To minimize this problem, we have used the OneLoop implementation of the scalar integrals,  $B_0$ ,  $C_0$ , and  $D_0$ . Even with this implementation, we have faced numerical instabilities in the evaluation of pentagon-tensor integrals<sup>1</sup>. This is related to inaccurate evaluation of Gramm determinants for certain phase-space points. These are the phase-space points where linear independency of external momenta (modulo 4-momentum conservation) does not hold to a very good accuracy. Indeed they lie on the kinematic boundaries of various channels. We judiciously throw away such points by making a gauge invariance test on the full amplitude. Since such points are few, given the nature of the integral evaluation, we don't expect significant impact of this aspect of the calculation. This is a common practice in such loop calculations. More complete discussion on this can be found in [32, 33].

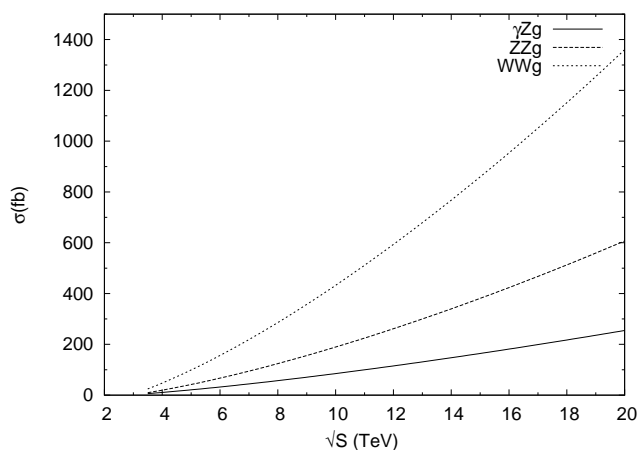


Figure 2: Variation of the cross-section with the centre-of-mass energy for  $gg \rightarrow VV'g$ .

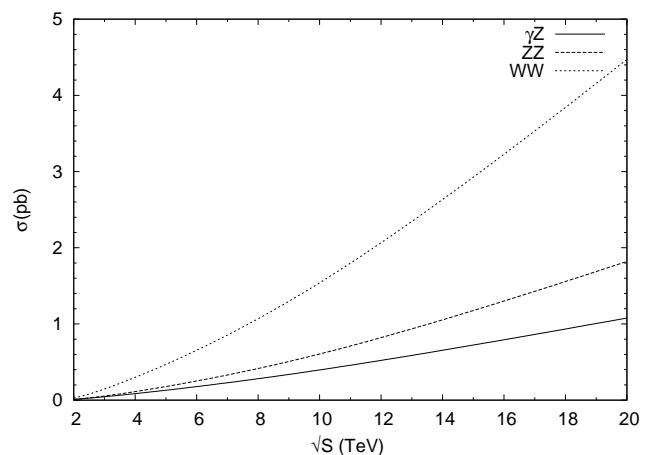


Figure 3: Variation of the cross-section with the centre-of-mass energy for  $gg \rightarrow VV'$ .

In Fig. (2), we present the results of the cross-section calculation for three processes. These results include following kinematic cuts:

$$P_T^{\gamma,Z,W,j} > 30 \text{ GeV}, |\eta^{\gamma,Z,W,j}| < 2.5, R(\gamma, j) > 0.6.$$

We have also chosen factorization and renormalization scales as  $\mu_f = \mu_R = P_T^{\gamma/Z/W}$ , as appropriate. We have used CTEQ6M parton distribution functions to obtain these results [34]. We note that at typical LHC energy, the cross-sections would be of the order of 100 fb. For example, at the centre-of-mass energy of the 8 TeV, the cross sections are 46.7 fb, 95.5 fb, and 225.2 fb respectively for the  $\gamma Zg$ ,  $ZZg$  and  $W^+W^-g$  production. Therefore, one may expect a few thousand of such events at the end of present run. But a W/Z boson is observed through its decay channels. If we consider the case when all the W/Z bosons are seen through their decays to the electron/muon only, then, with  $20 \text{ fb}^{-1}$  integrated luminosity, the number of events for these processes will be approximately 60, 10, and 220 respectively. However, if we allow one of the W/Z boson to decay hadronically, then the number of

<sup>1</sup> We would like to emphasize that we have also calculated di-vector boson production via gluon fusion for comparison as discussed below. These processes involve tensor integrals up to box type only and we have not faced any numerical instability in the calculation. The reduction method adopted in our calculation is indeed very stable numerically.

events would increase significantly. At the 14 TeV centre-of-mass energy, the numbers will be about a factor of three larger. The relative behavior of cross-sections of the three processes, as the center-of-mass energy varies, is quite similar to the case of di-vector boson production via gluon fusion as shown in Fig. (3). This common behavior is mainly due to the relative couplings of the processes listed above in (3). We find that at 14 TeV the cross-sections for our processes are 20 – 30% of those for corresponding di-vector boson production (without jet) processes. We can also compare the contribution of the loop processes with the tree-level processes. We find that the processes  $gg \rightarrow \gamma Zg, W^+W^-g$  make about 4 – 5% contribution to the processes  $pp \rightarrow \gamma Zj, W^+W^-j$ , while  $gg \rightarrow ZZg$  makes a contribution of about 10 – 15% to the  $pp \rightarrow ZZj$  process. Here ‘j’ stands for a jet. This is quite similar to the case of di-vector boson production. Tree level estimates are obtained using MadGraph [35]. We have also compared our results for the  $W^+W^-j$  production with those of *Melia et al.* [20]. Though they have considered the leptonic decays of  $W$ -bosons and kinematic cuts, choice of scales and parton distributions etc are quite different, the percentage contribution of gluon-gluon channel as compared to the LO cross-section is same within the allowed range of uncertainty, *i. e.* 4 – 5%. The values of the cross-section are more strongly dependent on the values of parameters and kinematic-cuts; still two results are similar if we take into account quoted uncertainties and branching ratios. The contribution of these gluon fusion processes can be even larger in appropriate kinematic regime.

We now discuss few kinematic distributions at 8 TeV collider centre-of-mass energy. These distributions remain same, characteristically, at 14 TeV centre-of-mass energy. The invariant mass distributions for pairs of vector boson are shown in Fig. (4). The positions of the peaks are related to the masses of the vector bosons in each case. In Fig. (5) the transverse momentum distributions for gluon is given for three processes. The major contribution to the cross-section comes from low  $P_T$  region, as we expect. The cross-section is very sensitive to  $P_T$  cut on gluon as it can come from one of the incoming gluons in the box contribution. We have compared the  $P_T$  distributions of  $\gamma$  and  $g$  for the case of  $\gamma Zg$  in Fig. (6). The rapid fall of  $P_T^g$  distribution compared to that of  $P_T^\gamma$  can be seen clearly. This is because the photon is coming from the quark loop, rather than from a quark-leg (as in the case of tree-level process). A larger cut on this transverse momentum will enhance the relative contribution of the loop process.

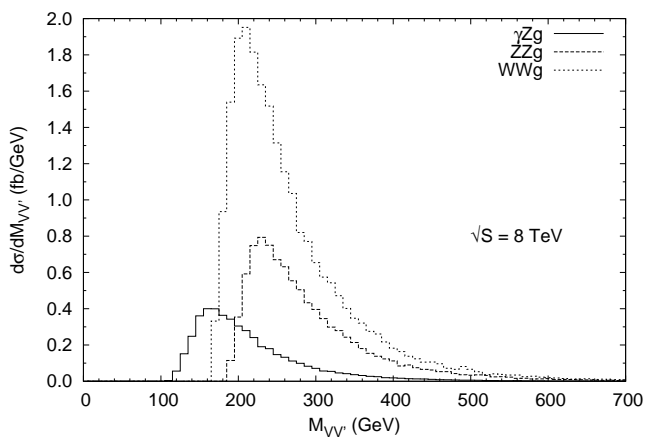


Figure 4: Invariant Mass distribution of vector boson pairs at 8 TeV.

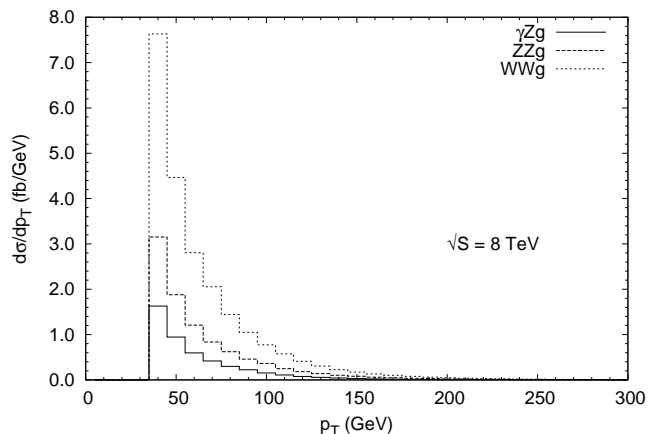


Figure 5: Transverse momentum distribution of Gluons at 8 TeV.

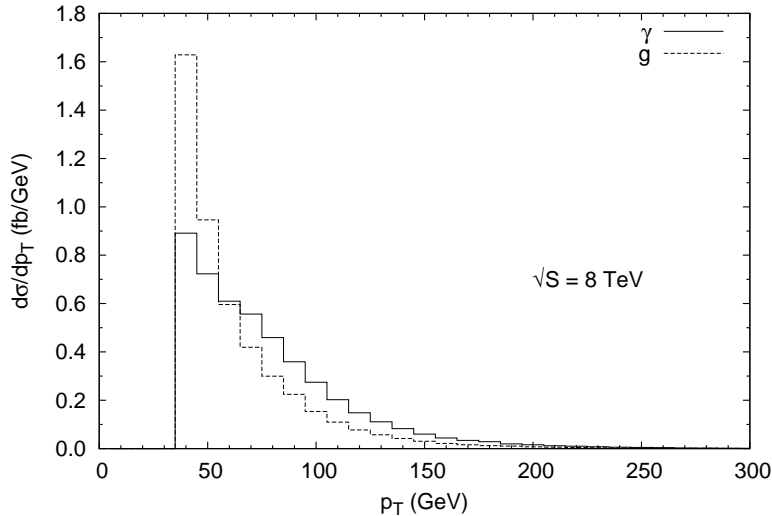


Figure 6: Comparison of  $P_T$  distributions of  $\gamma$  and  $g$  for  $\gamma Zg$  production at 8 TeV.

## 5 Conclusions

We have presented the results of the cross-section calculations for the processes  $gg \rightarrow \gamma Zg, ZZg$  and  $W^+W^-g$ . These are one-loop processes and proceed via pentagon and box diagrams. We have kept only  $\gamma Zg$  like contributions for the cases of  $ZZg$  and  $WWg$ . There is decoupling of the top-quark. For the  $WWg$  case, the contribution from the first two generations of the quark is included. We have made a number of checks on our calculation. We have verified the cancellation of UV and mass singularities. We have also checked gauge invariance with respect to all the gauge particles. Axial-vector contribution does not interfere with the vector contribution and it is separately gauge invariant. We have observed qualitative similarity of these processes with the corresponding di-vector boson production cases. All these processes have already generated several hundred events at the LHC. In appropriate kinematic regime one should be able to observe these processes. The contribution of the process  $gg \rightarrow ZZg$  is specially significant. It may have bearing on the searches of the Higgs boson and new physics scenarios that lead to two Z-boson in the final state. Detailed and more complete study of these processes will be reported in future publications.

AS would like to acknowledge fruitful discussions with R. Frederix and D. Zeppenfeld. He would also like to thank Dr. S. Veseli for his help with AMCI package.

## References

- [1] <http://press.web.cern.ch/press/PressReleases/Releases2012/PR17.12E.html>
- [2] Andy Parker, *SUSY Searches (ATLAS/CMS)*; Steven Worm, *Searches for Beyond the Standard Model* (talks given at ICHEP 2012, Melbourne, Australia)
- [3] L. Ametller, E. Gava, N. Paver and D. Treleani, Phys. Rev. D **32**, 1699 (1985).
- [4] D. A. Dicus, C. Kao and W. W. Repko, Phys. Rev. D **36**, 1570 (1987).

- [5] D. A. Dicus and S. S. D. Willenbrock, *Phys. Rev. D* **37**, 1801 (1988).
- [6] J. J. van der Bij and E. W. N. Glover, *Phys. Lett. B* **206**, 701 (1988).
- [7] E. W. N. Glover and J. J. van der Bij, *Nucl. Phys. B* **321**, 561 (1989).
- [8] E. W. N. Glover and J. J. van der Bij, *Phys. Lett. B* **219**, 488 (1989).
- [9] T. Matsuura and J. J. van der Bij, *Z. Phys. C* **51**, 259 (1991).
- [10] C. Zecher, T. Matsuura and J. J. van der Bij, *Z. Phys. C* **64**, 219 (1994) [hep-ph/9404295].
- [11] T. Binoth, M. Ciccolini, N. Kauer and M. Kramer, *JHEP* **0503**, 065 (2005) [hep-ph/0503094].
- [12] T. Binoth, M. Ciccolini, N. Kauer and M. Kramer, *JHEP* **0612**, 046 (2006) [hep-ph/0611170].
- [13] P. M. Nadolsky *et al.*, *Phys. Rev. D* **76**, 013008 (2007) [hep-ph/0702003 [HEP-PH]].
- [14] T. Binoth, N. Kauer and P. Mertsch, arXiv:0807.0024 [hep-ph].
- [15] J. M. Campbell, R. K. Ellis and C. Williams, *JHEP* **1107**, 018 (2011) [arXiv:1105.0020 [hep-ph]].
- [16] J. M. Campbell, R. K. Ellis and C. Williams, *JHEP* **1110**, 005 (2011) [arXiv:1107.5569 [hep-ph]].
- [17] D. de Florian and Z. Kunszt, *Phys. Lett. B* **460**, 184 (1999) [hep-ph/9905283].
- [18] P. Agrawal and G. Ladinsky, *Phys. Rev. D* **63**, 117504 (2001) [hep-ph/0011346].
- [19] P. Agrawal and A. Shivaji, *PoS (RADCOR2011) 010* [arXiv:1201.0511 [hep-ph]]; P. Agrawal, *Multi-Vector Boson Production via Gluon-Gluon Fusion* (talk given at PLHC 2012, Vancouver, Canada )
- [20] T. Melia *et al.*, *JHEP* **1208**, 115 (2012) [arXiv:1205.6987 [hep-ph]].
- [21] M. E. Peskin and D. V. Schroeder, *An Introduction to Quantum Field Theory (Paperback)*, **Levant Books, 2005**
- [22] J. A. M. Vermaseren, *math-ph/0010025*.
- [23] G. J. van Oldenborgh and J. A. M. Vermaseren, *Z. Phys. C* **46** (1990) 425.
- [24] W. L. van Neerven and J. A. M. Vermaseren, *Phys. Lett. B* **137**, 241 (1984).
- [25] A. van Hameren, *Comput. Phys. Commun.* **182**, 2427 (2011) [arXiv:1007.4716 [hep-ph]].
- [26] R. Kleiss, W. J. Stirling and S. D. Ellis, *Comput. Phys. Commun.* **40**, 359 (1986).
- [27] G. 't Hooft and M. J. G. Veltman, *Nucl. Phys. B* **153**, 365 (1979).
- [28] G. Duplancic and B. Nizic, *Eur. Phys. J. C* **20**, 357 (2001) [hep-ph/0006249].
- [29] T. Appelquist and J. Carazzone, *Phys. Rev. D* **11**, 2856 (1975).
- [30] S. Veseli, *Comput. Phys. Commun.* **108**, 9 (1998).
- [31] Message Passing Interface Forum, *Int. J. Supercomp. Apps.* **8**, **157** (1994)



- [32] P. Agrawal and A. Shivaji, arXiv:1208.2593 [hep-ph].
- [33] F. Campanario, JHEP **1110**, 070 (2011) [arXiv:1105.0920 [hep-ph]].
- [34] P. M. Nadolsky *et al.*, Phys. Rev. D **78**, 013004 (2008) [arXiv:0802.0007 [hep-ph]].
- [35] J. Alwall *et al.*, JHEP **1106**, 128 (2011) [arXiv:1106.0522 [hep-ph]].